Phosphomimetics at Ser199/Ser202/Thr205 in Tau Impairs Axonal Transport in Rat Hippocampal Neurons

Kyle R. Christensen[1,2] · Benjamin Combs[1] · Collin Richards[1] · Tessa Grabinski[1] · Mohammed M. Alhadidy[1,2] · Nicholas M. Kanaan[1,2,3]

Abstract

Our understanding of the biological functions of the tau protein now includes its role as a scaffolding protein involved in signaling regulation, which also has implications for tau-mediated dysfunction and degeneration in Alzheimer's disease and other tauopathies. Recently, we found that pseudophosphorylation at sites linked to the pathology-associated AT8 phosphoepitope of tau disrupts normal fast axonal transport through a protein phosphatase 1 (PP1)-dependent pathway in squid axoplasm. Activation of the pathway and the resulting transport deficits required tau's N-terminal phosphatase-activating domain (PAD) and PP1 but the connection between tau and PP1 was not well defined. Here, we studied functional interactions between tau and PP1 isoforms and their effects on axonal transport in mammalian neurons. First, we found that wild-type tau interacted with PP1α and PP1γ primarily through its microtubule-binding repeat domain. Pseudophosphorylation of tau at S199/S202/T205 (psTau) increased PAD exposure, enhanced interactions with PP1γ, and increased active PP1γ levels in mammalian cells. Expression of psTau also significantly impaired axonal transport in primary rat hippocampal neurons. Deletion of PAD in psTau significantly reduced the interaction with PP1γ, eliminated increases of active PP1γ levels, and rescued axonal transport impairment in neurons. These data suggest that a functional consequence of phosphorylation within S199-T205 in tau, which occurs in AD and several other tauopathies, may be aberrant interaction with and activation of PP1γ and subsequent axonal transport disruption in a PAD-dependent fashion.

Abbreviations

AD	Alzheimer's disease
CNS	Central nervous system
C-term	C-terminus
ΔC-term	C-terminus deleted
GSK3β	Glycogen synthase kinase-3β
HT	HaloTag
HEK	Human embryonic kidney
IDPs	Intrinsically disordered proteins
MTBRs	Microtubule binding repeats
N-term	N-terminus
ΔN-term	N-terminus deleted
NLuc	Nano-Luciferase
PAD	Phosphatase activating domain
PP1	Protein phosphatase 1
PP1c	Protein phosphatase 1 catalytic subunit
psTau	Pseudophosphorylated tau protein at serine 199, serine 202, and threonine 205
WT	Wild-type (hT40) tau protein

Kyle R. Christensen and Benjamin Combs contributed equally to this work.

✉ Nicholas M. Kanaan
nkanaan@msu.edu

1. Department of Translational Neuroscience, Michigan State University, 400 Monroe Ave NW, Grand Rapids, MI 49503, USA

2. Neuroscience Program, Michigan State University, East Lansing, MI 48824, USA

3. Hauenstein Neuroscience Center, Mercy Health Saint Mary's, Grand Rapids, MI 49503, USA

Introduction

Tau is a microtubule-associated protein and traditionally associated with a role in regulating microtubule dynamics [1, 2]. However, tau also regulates localization and, potentially, the activity of multiple signaling molecules (reviewed in [3]). For example, tau may promote NGF-mediated MAPK signaling by activating MAPK in cells [4, 5] or modulate Fyn kinase localization and activity [6–8]. Recently, we demonstrated a functional interaction between wild-type tau and protein phosphatase 1 (PP1) that was associated with activation of the phosphatase [9]. This aligned with previous work by Liao and colleagues that demonstrated tau interacts with PP1 in blot overlay assays and targets PP1 to microtubules [10]. Thus, tau's functional repertoire appears much larger than modulating microtubule dynamics and may include cell signaling functions [3], including regulation of PP1.

PP1 is a member of the serine/threonine protein phosphatase family, one of the most highly conserved protein families with ubiquitous expression in eukaryotes [11]. PP1 is involved in several cellular functions including cytoskeletal reorganization, membrane channel regulation, axonal transport, and many others [11, 12]. The phosphatase exists as a holoenzyme complex comprised of its catalytic subunit (PP1c) and one or more regulatory proteins. There are over 200 PP1c regulatory proteins, allowing for the broad context of its functions [13, 14]. Three genes encode the PP1c isoforms: *PPP1CA* (PP1α), *PPP1CB* (PP1β), and *PPP1CC* (PP1γ). Alternative splicing of *PPP1CC* produces two isoforms, PP1γ$_1$ and PP1γ$_2$, with PP1γ$_1$ being more prevalent in the central nervous system (CNS) [15–17]. Variations between the isoforms exist in the N- and C-termini, while the catalytic core is highly conserved [18, 19]. Most regulatory proteins interact with PP1 through the RVxF binding motif [20, 21], of which tau has three similar motifs, including one in the N-terminus (amino acids 5–8) and two in the microtubule binding repeats (MTBRs; amino acids 343–346 and 375–378) [10].

A growing body of evidence suggests that many disease-related modifications of tau disrupt axonal transport through a mechanism involving an N-terminal motif called the phosphatase-activating domain (PAD, amino acids 2–18) and its activation of a PP1-dependent pathway. Axonal dysfunction and degeneration is observed in Alzheimer's disease (AD) and other related neurodegenerative disorders, representing a site of potential toxic mechanisms in these diseases [22]. In tauopathies, abnormal modifications of tau, including phosphorylation of specific epitopes and oligomerization, alter tau conformation and are associated with exposure of PAD during early stages of the accumulation of pathological tau (e.g. in pre-tangle neurons) [23–27]. Phosphorylation of tau at AT8 phosphoepitope sites (S199, S202 and T205) [28, 29] is another early and prominent modification associated with AD pathology [24, 27, 30–34]. Previous studies using structural FRET analysis showed that phosphomimicking specifically at the combination of Ser199/Ser202/Thr205 (psTau, using S/T to E mutations) disrupts the "paperclip" conformation causing an extension of the N-terminus out of the paperclip conformation in soluble monomeric proteins, potentially exposing the PAD [23]. The same psTau monomeric protein inhibits anterograde fast axonal transport in the squid axoplasm model [24]. Additionally, individual and combinatorial phosphomimetic mutations within the psTau sites also inhibited fast axonal transport in squid axoplasms [35]. In both cases PAD-related conformation changes and PP1-initiated signaling pathways mediated the inhibitory effects [24, 35]. Additionally, tau phosphorylated at Thr205 co-localized with PAD-exposed tau in the axonal growth cone and PAD was required for tau-mediated rescue of neurite outgrowth dysfunction in developing tau knockout primary neuron cultures [36]. Recently, our group showed that two mutant forms of tau that cause inherited tauopathy (i.e. P301L and R5L mutations) also impair transport through a PAD- and PP1γ-dependent mechanism in mammalian primary neurons [9]. Together, these data suggest a toxic cascade whereby disease-related tau modifications induce a conformation change that alters its functional interactions with PP1 and leads to disruption of axonal transport in neurons. However, prior studies in mammalian neurons used inherited tau mutations and did not establish whether disease-related phosphorylation patterns in wild-type tau (e.g. psTau) also alter functional interactions with PP1 and the consequences of those changes on axonal transport.

Here, we characterized the protein–protein interaction between tau and the PP1 isoforms and determined the tau-induced effects on levels of active PP1. Then we examined the effects of the psTau modification on PAD exposure and functional interactions with PP1. We found that tau interacts with PP1α and PP1γ primarily through the MTBR domain and full-length WT tau increased levels of active PP1. The psTau modification induced PAD exposure and significantly enhanced interaction with PP1. The psTau-induced increases in active PP1 levels were dependent upon PAD. Functionally, psTau caused axonal transport abnormalities (i.e. increased pause frequency) in primary rat hippocampal neurons that were rescued by deletion of PAD. These findings support the idea that tau may physiologically modulate PP1 and that the disease-associated phosphorylation in the S199-T205 region of tau causes PP1 dysregulation and axonal transport impairment in mammalian neurons that is dependent upon the presence of PAD.

Materials and Methods

Tau and PP1 Constructs

Tau proteins sequences are designated by the longest human tau isoform in the CNS (hT40 or 2N4R, 441 amino acids). This tau isoform contains both N-terminal exons and four microtubule binding repeat regions (MTBRs) and here we refer to this as wild-type (WT) tau. Tau domain constructs corresponding to the different regions in the tau protein were generated to assess how the specific regions of tau interact with PP1 (Fig. 1). The N-terminus domain (N-Term) contains amino acids 1–224, the MTBR domain (MTBR) contains the four MTBRs and is composed of amino acids 225–380, the C-terminus domain (C-Term) contains amino acids 381–441, the deletion of the C-terminus (ΔC-Term) is composed of amino acids 1–380, and the deletion of the N-terminus (ΔN-Term) is composed of amino acids 225–441. Point mutations in WT tau were performed to mutate S199, S202, and T205 to glutamic acid to mimic phosphorylation at the AT8 epitope (psTau). Finally, the PAD (amino acids 2–18) was deleted from these constructs to assess the role of PAD in modulating PP1 interactions and activity (ΔPAD WT and ΔPAD psTau). PP1 constructs included human PP1α or PP1γ1 isoform cDNA sequences.

HaloTag Pulldown Assays

Human embryonic kidney (HEK) 293 T (ATCC CRL-3216; RRID:CVCL_0063) cells were transfected with Tau and PP1 constructs under control of a pCMV promoter. Tau protein was fused to NanoLuciferase (NLuc) tag and PP1 was fused to HaloTag (HT, Promega HaloTag System G6051) [37]. HEK 293 T cells were grown in DMEM (Thermo 11995–065) supplemented with 5% FBS and 1% penicillin/streptomycin (Thermo 15140–122) in a humidified incubator at 37° and 5% CO_2. Cells were plated in a 12-well plate at 300,000 cells/well in 1 mL DMEM (supplemented with 5% FBS and 1% penicillin/streptomycin) one day prior to transfection. Cells were co-transfected with 500 ng each of pCMV tau-NLuc fusion construct and pCMV HT-PP1 isoform fusion constructs using Lipofectamine 2000 (Invitrogen 52887) according to the manufacturer's instructions and incubated overnight. The next day, cells were collected in lysis buffer (50 mM Tris–HCl, 150 mM NaCl, 1% Triton X-100, 10 μg/mL pepstatin, 10 μg/mL leupeptin, 10 μg/mL bestatin, 10 μg/mL aprotinin, 1 mM PMSF, pH 7.5) and dounce homogenized. Homogenates were centrifuged at 14,000×g for 5 min at 4° C to pellet debris, and the supernatant was transferred to a new tube. Lysates were diluted in TBS to bring the Triton X-100 to 0.3%. 12.5 μl of lysate was removed as the input fraction (Input). 50 μl HaloLink resin (Promega G1915) was equilibrated in Halo Wash Buffer (50 mM Tris–HCl, 150 mM NaCl, 0.05% NP-40, pH 7.5) by washing three times in 500 μl wash buffer. Resin was centrifuged at 800×g for 2 min at room temperature after each wash to settle resin and allow for aspiration of the supernatant. After removing the last wash buffer, 450 μl lysate was added to resin and incubated for one hour at room temperature with end-over-end mixing. Resin was pelleted via centrifugation, and the supernatant saved as the post-pulldown flow through fraction (Post). The resin was washed four times with Halo Wash Buffer, and bound proteins were eluted by incubating in 50 μl of 2×Laemmli Sample Buffer (40 mM Tris pH 6.8, 3.3% SDS, 10.7% glycerol, 2.5% β-mercaptoethanol, 0.004% bromophenol blue) for 30 min at 30 °C and 1000 RPM shaking. Resin was pelleted via centrifugation, and the resulting supernatant was saved as the elution fraction for western blot analysis.
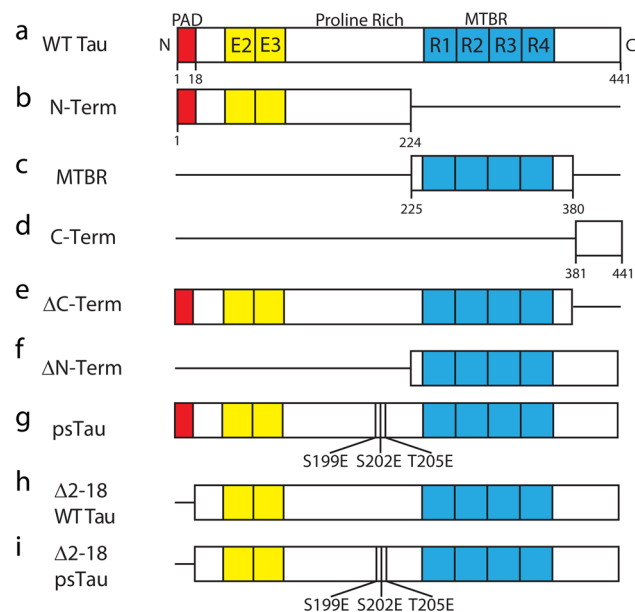

Fig. 1 Schematic of tau constructs used in this study. **a** Full-length wild-type hT40 (WT Tau, 441 amino acids) containing the PAD region at amino acids 2–18 (red box), exons 2 and 3 in the N-terminus (E2 and E3, yellow boxes), the proline rich region, and four microtubule binding repeat regions (MTBRs, R1-R4, blue boxes). **b** N-terminus domain (N-Term) of WT tau corresponding to amino acids 1–224. **c** MTBR domain of WT tau corresponding to amino acids 225–380. **d** C-terminus domain (C-Term) of WT tau corresponding to amino acids 381–441. **e** Protein with deletion of the C-terminus (ΔC-Term) corresponds to amino acids 1–380. **f** Protein with deletion of the N-terminus (ΔN-Term) corresponds to amino acids 225–441. **g** WT tau was pseudophosphorylated by mutating S199, S202, and T205 into glutamic acid (psTau) to mimic the AT8 phosphoepitope. **h** WT tau with the PAD region removed (Δ2-18 WT). **i** psTau with the PAD region removed (Δ2-18 psTau). All tau constructs were C-terminally tagged with either a 6xHis tag for recombinant tau purification or NanoLuciferase for use in the Halo pulldown assays and NanoBRET in-cell protein interaction assays

NanoBRET Assays

HEK 293 T cells were plated in a 12-well plate at a density of 400,000 cells/well in 1 ml plating volume. Six hours later, cells were co-transfected with a pCMV tau-NLuc fusion construct (donor) and a pCMV HT-PP1 construct (acceptor) with Lipofectamine 2000. Donor saturation curve experiments were performed previously with WT tau and PP1α, PP1β or PP1γ and demonstrated the specificity of the interaction between tau and PP1 isoforms in NanoBRET assays [9]. Here, single ratio NanoBRET assays were performed with an optimized DNA ratio of 1:30 (10 ng donor DNA and 300 ng acceptor DNA). An empty plasmid was used as a carrier DNA to standardize transfection amounts. After transfection, cells were incubated overnight. The next day cells were replated in triplicate into a white-wall, clear-bottom 96-well plate with a 618 nm fluorescent ligand that covalently binds to HT or DMSO as a control according to the manufacturer's instructions (Promega NanoBRET Nano-Glo Detection System N1661) [37]. Replated cells were incubated overnight. The next day, the cell culture media was removed and replaced with 100 μl fresh media to remove unbound 618 nm ligand before Nano-Glo substrate was added to each well according to the manufacturer's instructions. Donor luminescence and acceptor fluorescence was measured on a BioTek Synergy H1 microplate reader using a 460/40 nm bandpass filter and a 610 nm longpass filter respectively. NanoBRET ratios were calculated by dividing the acceptor signal by the donor signal and subtracting the ratios from the no-ligand DMSO controls.

Recombinant Protein Production

All tau constructs were expressed in *Escherichia coli* using the pT7c backbone and fused to a 6×histidine tag for purification. The histidine tag was present on the C-terminus for each tau construct. Recombinant proteins were purified on an Akta Pure 25L fast protein liquid chromatography machine (GE Healthcare 29018224) by immobilized metal affinity chromatography using a HiTrap TALON Crude column (GE Healthcare 28953767) as described previously [38]. Tau protein purifications were followed by size exclusion chromatography over an S500 column (GE Healthcare 28–9356-06) and anion exchange chromatography over a HiTrap Q HP column (GE Healthcare 17–1154-01) [38]. DTT was added to a final concentration of 1 mM before aliquoting the purified tau proteins and storing at -80 °C. Protein concentrations were determined using the SDS-Lowry assay method as described [39].

Pulldown Western Blotting and Dot Blotting

Pulldown fractions (Input, Post, and Elution) were denatured at 98 °C for 5 min before being loaded onto a 4–20% Tris–HCl Criterion gel (BioRad 3450034) and proteins separated by SDS-PAGE. Proteins were transferred to a nitrocellulose membrane and probed with HaloTag antibody (1:1000, mouse monoclonal IgG1, Promega G9211; RRID:AB_2688011) to label PP1 proteins or HaloTag alone, and either NanoLuciferase (1:5000, rabbit polyclonal, Promega) or R1 (1:100,000, RRID:AB_2832929, rabbit polyclonal pan-tau antibody) [40] antibodies for the tau domains or full-length and ΔPAD tau proteins, respectively. Note that the HaloTag antibody displays some cross-reactivity with the N-terminus of tau proteins, but this does not interfere with clear interpretation of immunoblots due to migration differences in each protein of interest. Antibodies were diluted in 2% non-fat dry milk in TBS and blots were incubated overnight at 4 °C. The next day, blots were incubated for 1 h at room temperature with IRDye 800CW goat-anti-rabbit IgG (H + L) (1:20,000, LiCor Biosciences 925–32211, RRID:AB_2651127) and IRDye 680LT goat-anti-mouse IgG (H + L) (1:20,000, LiCor Biosciences 926–68020, RRID:AB_10706161). Blots were imaged using a LiCor Odyssey system. Band signal intensities were quantified using ImageStudio software and the Elution tau band intensities were normalized to efficiency of HaloTag affinity pulldown (i.e. difference between HaloTag signal in the Input and Post samples).

Recombinant tau proteins were analyzed using western blots and dot blots as described [24]. Briefly, 500 ng of WT tau and psTau recombinant proteins were used per spot or gel lane. Both blots were probed for R1 (as above) and TNT1 (1:200,000, RRID:AB_2736930) to detect PAD exposed tau [24]. The signal from TNT1 (PAD exposed tau) [24, 25, 39, 41] was normalized to R1 signal (total tau).

Phospho-PP1 Western Blotting

HEK 293 T cells were plated at a seeding density of 400,000 cells/well in a Poly-D-Lysine 12-well plate (Corning #354470). The next day, cells were transfected with N-Halo-tagged PP1γ along with either C-FLAG-tagged GFP, WT tau, Δ2-18 WT tau, psTau, or Δ2-18 psTau. For each transfection group, 2 tubes were prepared: tube 1 contained 100 μl of sterile-filtered 150 mM NaCl and 10 μl of PEI (Polysciences # 23966–1; stock concentration is 0.323 g/L). Tube 2 contained 100 μl of 150 mM NaCl and 1 μg total plasmid DNA (0.5 μg of each plasmid). Contents of tube 1 were transferred to tube 2, mixed well by vortex, and incubated at room temperature for 20 min. Then, 200 μl of PEI-DNA mixtures were added dropwise to each

well. On day 3, cells were lysed in-well using 150 µl of Co-IP buffer (20 mM Tris, pH 7.5; 0.5 mM DTT; 0.15 M NaCl; 0.5% Triton X-100) supplemented with protease inhibitors (pepstatin, bestatin, leupeptin, PMSF, and aprotinin) and phosphatase inhibitors (sodium fluoride, sodium orthovandate, β-glycerophosphate, and sodium pyrophosphate decahydrate). Cell lysates were sonicated with 4 pulses, 5 s each, followed by centrifugation at 12,000xg for 10 min at 4 degrees. Protein concentration in supernatant was quantified using Bradford assay (Biorad #5000006). Supernatants were loaded for SDS-PAGE (40 µg total protein) and Western blotting as described above. The membranes were probed with primary antibodies: GFP (1:30,000. Abcam #ab290, RRID:AB_303395), pT320 PP1α (1:500, Cell Signaling Technology #CST2581, RRID:AB_330823), Halo (1:1,000, Promega #G9211, RRID:AB_2688011), and Tau5 (1:100,000, RRID:AB_2721194) followed by secondary antibodies: IRDye 800CW goat-anti-rabbit IgG (H + L) (1:20,000, LiCor Biosciences 925–32211, RRID:AB_2651127) and IRDye 680LT goat-anti-mouse IgG (H + L) (1:20,000, LiCor Biosciences 926–68020, RRID:AB_10706161). Membranes were then re-probed with GAPDH antibody (1:2,000, RRID:AB_10622025, Cell Signaling Technology, CST #5174) and the Goat anti-Rabbit secondary antibody.

Animals and Primary Neuron Culture

Timed-pregnant Sprague–Dawley rats (Envigo) were used to obtain embryonic day 18 (E18) fetuses. Primary hippocampal neuron cultures were prepared from the fetuses using previously described methods [42]. Briefly, hippocampi were dissected from the rat embryos and incubated in 0.125% trypsin for 15 min and 37 °C. Trituration using progressively smaller needles was used to dissociate tissue and the cells were plated in antibiotic-free neurobasal media.

Axonal Transport Assays

Primary hippocampal neurons were plated at 80,000 cells/well into 4-well live cell chamber slides (Ibidi, #80427) coated with poly-D-lysine (Sigma-Aldrich P7886) in 750 µl of neurobasal media (Gibco, #21103049) supplemented with GlutaMAX (Gibco, #35050061) and B27 (Gibco, #17504044). On day *in vitro* (DIV) 8 the cells were transfected using Lipofectamine 2000 reagents. Each transfection included 200 ng each of pFIN Synaptophysin-mApple and a plasmid containing the tau construct (WT tau, psTau, Δ2-18 WT tau, or Δ2-18 psTau) or a GFP control protein in 30 µl of Opti-MEM serum-free media. 0.5 µl of Lipofectamine2000 was

incubated in 30 µl of Opti-MEM media for 30 min at room temperature for each condition. The Lipofectamine mix was added to the DNA mix and incubated for an additional 30 min. 60 µl of sample was added dropwise throughout the entirety of the well. After two hours, half of the media (380 µl) was replaced with an equivalent volume of neurobasal media containing an antibody that binds the extracellular domain of neurofascin in the axon initial segment (250 ng/ml, UC Davis/NIH NeuroMab #75–172, RRID:AB_2282826) [43]. At 24 h post-transfection, all media was replaced by neurobasal media containing Alexa Fluor goat-anti mouse IgG2a 647 antibody (1:2,000, ThermoFisher A-21241, RRID:AB_2633277).

After a one-hour incubation the neurons were imaged on the Nikon A1 + laser scanning confocal microscope equipped with 488, 561, and 640 solid state lasers using a 60x/1.40 NA objective and Nikon Elements AR software. The plates were maintained in a live cell chamber at 37 °C and 5% CO_2 throughout the imaging process. Regions of analysis were identified in a main branch of the axon and 50 to 150 µm from the axon initial segment. A region of 32 pixels by 128 pixels was bleached with 7 pulses of 1.7 s each from a 568 nm laser at 60% power. After 2 min movement of the mApple-synaptophysin cargo in the region was imaged at ~ 28 fps for 5 min using the 568 nm laser. The ImageJ macro KymoAnalyzer was used to generate and analyze kymographs [44]. The traces were identified manually. Anterograde and retrograde segment velocities represent a mean of each segment with a velocity faster than 0.3 µm/second. Pause frequency was determined as the number of pauses/track/second. Each individual replicate in the primary neuron experiments represents the mean value from all analyzed kymographs within a given primary neuron preparation and represent completely independent culture runs from different pregnant females. A minimum cutoff of 30 detectable tracks per kymograph was established. GFP: $n = 6$, 15 total neurons; WT tau: $n = 5$, 8 total neurons; psTau: $n = 5$, 6 total neurons; Δ2-18 WT tau: $n = 5$, 10 total neurons; Δ2-18 psTau: $n = 5$, 6 total neurons.

Statistical Analysis

All data and statistical analyses were performed using GraphPad Prism 7.0 software. Results were analyzed by unpaired t-test, one-way ANOVA with Tukey's post hoc test, or two-way ANOVA with Tukey's post hoc test as indicated in figure legends. For the repeated measures one-way ANOVAs used to quantify the PP1 western blots in Fig. 4, we used the Geisser–Greenhouse correction to account for violations of the assumptions of sphericity (as indicated here by an ε value < 0.5). The number

of independent experimental runs are indicated in figure legends and the significance level was set at $p \leq 0.05$ for all tests.

Results

The MTBR Domain of Tau Mediates the Interaction with PP1α and PP1γ

Previously, we identified a protein–protein interaction between WT tau protein and the PP1α and PP1γ isoforms, but little to no interaction with the PP1β isoform across multiple assays [9]. First, we pulled down HaloTag-PP1 fusion proteins from cell lysates and probed for WT tau, finding similar levels of tau co-elution with PP1α and PP1γ but not PP1β

[9]. Results from intracellular NanoBRET assays supported the same PP1 isoform-specific data from the pulldown assay [9]. Finally, we utilized a proximity ligation assay to confirm endogenous PP1 association with WT human tau, as well as endogenous rat tau, in primary rat hippocampal neurons [9]. After establishing a WT tau-PP1 interaction, here we investigated how various tau domains influence the interaction with the PP1α and PP1γ isoforms. We divided tau into five domain constructs (Fig. 1) and co-transfected them with PP1α or PP1γ in HEK 293 T cells for use in protein interaction assays. The MTBR domain showed the strongest interaction with PP1γ when compared to WT tau and all other tau domain constructs in pulldown assays (Fig. 2). We observed similar results with PP1α (Fig. S1). Moreover, NanoBRET assays showed a similar significant increase in the interaction between the MTBR domain and PP1γ when compared to
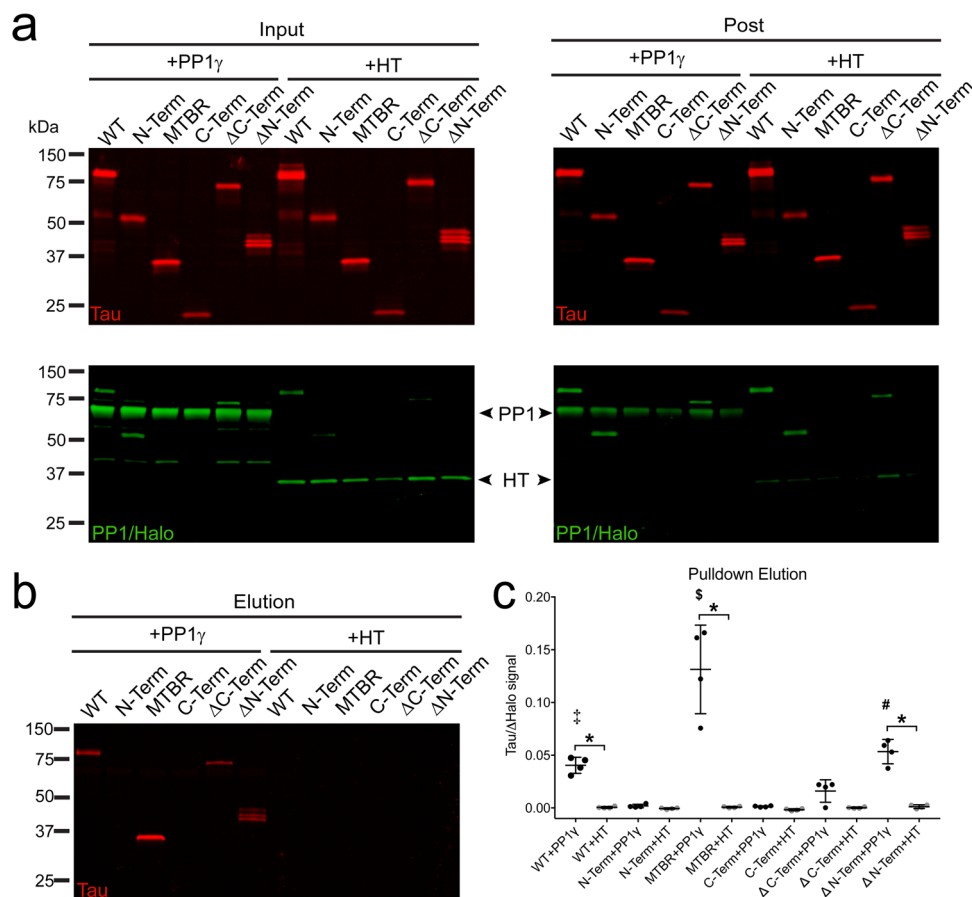

Fig. 2 The MTBR domain of WT tau is necessary and sufficient for interaction with PP1. HEK 293 T cells expressing each tau domain (tagged with NLuc) and PP1γ (tagged with HaloTag, HT) or HT only controls were used in pulldown assays. **a-b** Western blots of input samples (**a**, Input), post-pulldown flow-through samples (**a**, Post), and elution samples (**b**, Elution) are shown with PP1γ or HT in green and tau domains in red. **c** Quantification of tau signal in the elution sample shows significantly increased signal with the MTBR domain com-

pared to all other proteins, while deleting the N-terminus (ΔN-Term) or the C-terminus (ΔC-Term) did not significantly alter binding compared to full-length tau (WT). These experiments were repeated four independent times and all comparisons were made using a two-way ANOVA with Tukey's post hoc test (*$p \leq 0.05$ compared to HT control; $^{\$}p \leq 0.05$ compared to all other groups, $^{\ddagger}p \leq 0.05$ compared to N-Term and C-Term; $^{\#}p \leq 0.05$ compared to N-Term, C-Term and ΔC-Term)

other tau domains (Fig. S2a). Deletion of the N- or C-termini (ΔN-Term and ΔC-Term) of tau did not significantly alter interaction with PP1γ when compared to WT tau (Fig. 2) which suggests these regions are not essential for binding to PP1. The ΔC-Term and ΔN-Term proteins also showed significantly increased interaction with PP1γ when compared to the HT control in the NanoBRET assay (Fig. S2a).

Pseudophosphorylation of Tau Exposes PAD and Increases PP1γ Interaction

Previous work established that disease-related forms of tau (including the triple modified psTau and other single or double phosphomimics in this region) impair axonal transport in the squid axoplasm model and that tau-mediated inhibition of transport in this model is PP1-dependent [9, 24, 35, 45, 46]. However, the relationship between tau and PP1 was not directly explored with psTau. In previous FRET-based structural studies, the combination of phosphomimetics at S199/ S2020/T205 (psTau) causes extension of the N-terminus of tau that disrupts the paperclip conformation [23]; therefore, we hypothesized that psTau would expose the PAD region and promote an interaction between tau and PP1. Recombinant WT and psTau protein monomers were probed with the TNT1 antibody in a dot blot, a non-denaturing immunoblotting assay. TNT1 is a conformation-dependent monoclonal tau antibody that is established as a marker of PAD exposure [24, 25]. psTau displayed significantly more TNT1 reactivity when compared to WT tau (Fig. 3a) indicating increased PAD exposure. To confirm the sensitivity of TNT1 to conformational display of PAD, the same tau proteins were run in denaturing SDS-PAGE/Western blot assays. Denaturing the tau proteins eliminates the differential detection of PAD in psTau compared to WT tau (Fig. 3a), confirming that the psTau modification induces PAD-exposed conformations in soluble monomers as predicted based on prior FRET studies [23].
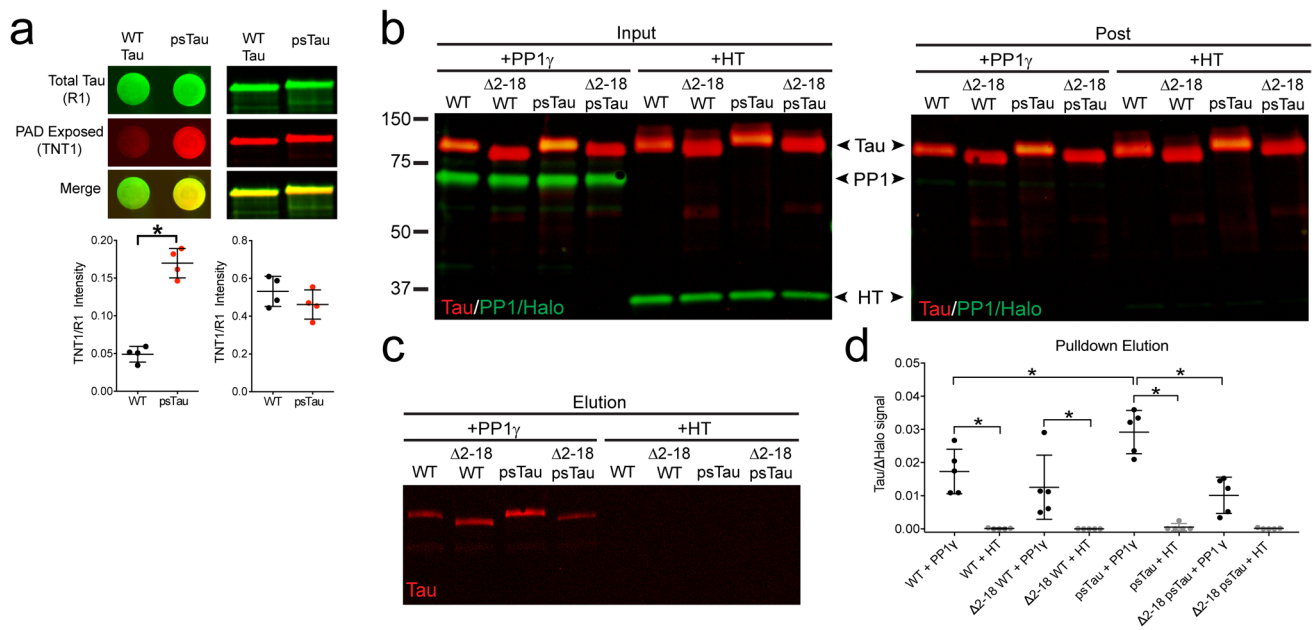

Fig. 3 psTau Exposes PAD and Increases the Interaction with PP1γ in PAD-dependent manner. **a** Recombinant human tau (WT tau) and psTau proteins were blotted using non-denaturing dot blots and denaturing western blots for TNT1 (a marker of PAD exposure in non-denaturing assays) and R1 (a pan-tau rabbit polyclonal antibody). Quantitation of blots indicate a significant increase in PAD exposure, as indicated by TNT1 reactivity, with psTau tau compared to WT tau (*$p \leq 0.05$ in an unpaired t-test). Data represent mean of normalized signal (TNT1 to R1 ratio) $\pm$ SD from four independent samples. A lack of significant differences in the denaturing western blot confirms that the TNT1 signal in the dot blots were due to conformational differences in the display of PAD. **b** HEK 293 T cells expressing each tau construct (tagged with NLuc) and PP1γ (tagged with HaloTag, HT) or HT only controls were used in pulldown assays. Western blots of starting lysate (Input) show similar expression of tau and PP1 constructs while post-pulldown samples (Post) confirm depletion of PP1γ and HT only controls. **c** Pulldown elution samples were probed for tau protein. All of the tested forms of tau eluted with pulldowns of PP1γ but none were present in pulldowns of the HT only controls. **d** Quantification of pulldown elution samples indicates that both WT and Δ2-18 WT tau showed a significantly increased interaction with PP1γ when compared to their respective HT only controls. Deletion of PAD from WT tau (Δ2–18 WT Tau) did not significantly affect the interaction with PP1γ. psTau showed a significantly increased interaction with PP1γ when compared to HT only controls and WT tau. Deletion of PAD in psTau (Δ2–18 psTau) significantly decreased the interaction with PP1γ compared to full-length psTau, and eliminated the increase compared to WT tau. The Δ2–18 psTau clearly interacted with PP1γ but interaction was a non-significant trend towards elevation above the HT control ($p = 0.075$). These experiments were repeated five independent times and data are mean $\pm$ SD. *$p \leq 0.05$ in a two-way ANOVA with Tukey's post hoc test

We next co-transfected HEK 293 T cells with WT tau or psTau and either PP1α or γ isoforms then compared the resulting interactions using the HaloTag pulldown and Nano-BRET assays. Both WT and psTau displayed an interaction with PP1γ that was above HT controls (Fig. 3b-d) and psTau further increased the interaction with PP1γ relative to WT in pulldown assays (Fig. 3c-d). In-cell NanoBRET assays confirmed that both WT tau and psTau interact with PP1γ (Fig. S2b). The psTau modification did not significantly change the interaction with PP1α when compared to WT tau in either assay (Fig. S3), thus, all remaining experiments with psTau focused on PP1γ.

PAD Modulates the Interaction and Activation of PP1γ by psTau

The PAD region, amino acids 2–18, inhibits anterograde fast axonal transport through a PP1-dependent mechanism in isolated squid axoplasm [24, 41, 45, 47], thus, we investigated the role of the PAD in tau-mediated interaction and activation of PP1γ. Deleting PAD (Δ2-18) from WT tau did not significantly change the interaction with PP1γ (Fig. 3c-d). However, deleting PAD from psTau significantly reduced the interaction with PP1γ in the pulldown assay (Fig. 3c-d), suggesting PAD plays a role in mediating the enhanced interaction effects due to the psTau modifications. Using the NanoBRET assay we confirmed an association between PP1γ and full-length and Δ2-18 versions of WT tau and psTau but none of these tau modifications significantly altered the tau-PP1 association in this experiment (Fig. S2c).

Next, we sought to determine how tau affected levels of active PP1 when co-expressed in HEK 293 T cells. We confirmed similar levels of tau expression (normalized to GAPDH) in the cells (Fig. 4a-b). By probing the cell lysates with a HaloTag antibody (Total PP1) and a phospho-PP1 antibody that detects the inactive form of the phosphatase (i.e. phosphorylated at T311 in PP1γ, corresponding to T320 in PP1α) [48, 49] we determined that WT tau and psTau expression increased levels of active PP1γ compared to GFP-expressing control cells, indicated by reduced inactive PP1γ levels (Fig. 4c-d). Deletion of PAD reduced this effect as indicated by
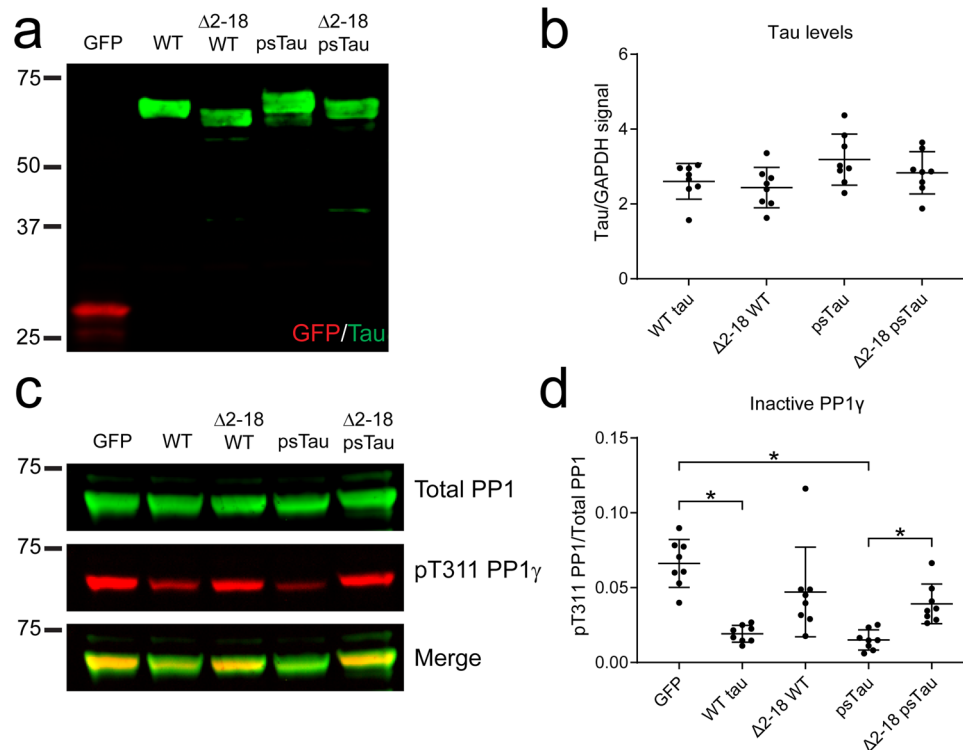

Fig. 4 PAD is necessary for psTau expression-induced increases to active PP1 levels in cells. **a** WT, Δ2-18 WT, psTau, Δ2-18 psTau, and GFP were individually transfected into HEK 293 T cells along with a PP1γ construct. Cells lysates were probed for tau and GFP expression. **b** Quantification of the blots confirmed similar levels of tau expression. **c** The lysates were also probed for Total PP1 (HT) and phospho-Thr311 PP1γ, the inactive form of the phosphatase. **d** Quantification of the blots identified increases in the levels of active PP1γ upon expression of WT tau and psTau compared to GFP expression (indicated by reductions in the proportion of inactive pT311 PP1γ to Total PP1). Deletion of amino acids 2–18 in psTau (Δ2-18 psTau) rescued the effect as levels of inactive PP1 were higher compared to psTau but not significantly different than in GFP-expressing cells. Data represent mean ± SD from 8 experiments and all comparisons were made using a repeated measures one-way ANOVA with a Geisser-Greenhouse correction and Tukey's post hoc test (*$p \leq 0.05$)

lower levels of active PP1γ (i.e., higher inactive pT311 PP1γ) with Δ2-18 psTau compared to expression of psTau (Fig. 4c-d). Neither of the Δ2-18 versions of tau significantly altered active PP1 levels compared to GFP expression (Fig. 4c-d). These data suggest that expression of tau induces an increase in active PP1γ compared to controls in a PAD-dependent manner.

psTau Disrupts Axonal Transport in Hippocampal Neurons in a PAD-dependent Fashion

Perfusion of psTau impairs anterograde axonal transport in the squid axoplasm model [24]. We took the next step of examining this effect in primary rat hippocampal neurons. We co-expressed a fluorescently-labeled synaptophysin cargo protein with either GFP, WT tau, psTau, Δ2-18 tau, or Δ2-18 psTau and imaged the cells using live-cell confocal microscopy at approximately 28 frames/sec (Fig. 5a, b). We used the KymoAnalyzer ImageJ macro to generate kymographs then manually marked the resulting tracks for analysis using the same program (Fig. 5c) [44].

We found that WT tau expression did not alter cargo velocity or pause frequency compared to expression of a GFP control protein (Fig. S4). This indicated that the axonal transport measurements used here were unaltered by WT tau. Next, we expressed WT or psTau to identify the transport effects due to phosphorylation at a pathogenic phospho-epitope and included Δ2-18 WT and Δ2-18 psTau to identify the role of PAD in the effects on transport. Expressing psTau increased anterograde segment velocity (cell body to synapse) compared to WT tau (38%) and both Δ2-18 forms of tau (Fig. 5d). The retrograde segment velocity (synapse to cell body) was not different among all groups (Fig. 5e). The presence of psTau significantly increased pause frequency of synaptophysin cargo in the anterograde direction (123%; Fig. 5f) and retrograde direction (87%: Fig. 5g) when compared to WT tau. Notably, deletion of PAD in psTau blocked the elevation in pause frequency in both directions (Fig. 5f, g). This demonstrates that the psTau modifications induce abnormal axonal transport in mammalian hippocampal neurons in a PAD-dependent fashion.

Discussion

Tau-Mediated Regulation of PP1

Recent evidence indicates tau may not only act as a substrate of PP1, but it also can regulate the localization and signaling functions of the phosphatase [9, 10, 24, 45]. We recently found an interaction between tau and the PP1α and PP1γ isoforms, but little to no interaction between WT tau and the PP1β isoform, using a combination of pulldown and in-cell interactions assays [9]. All three PP1 isoforms are expressed in neurons and display different subcellular enrichment, but each of the isoforms are present in axons and synaptic terminals [50, 51]. PP1α is expressed throughout the soma and processes (dendrites and axons), PP1β is more prevalent in the cell body, and PP1γ more prevalent in dendritic spines and presynaptic terminals [15, 50]. Although subcellular fractionation experiments indicate that PP1β is closely associated with axonal microtubules, the evidence suggests PP1β first interacts with a cell body-enriched interacting partner that targets it to microtubules [50]. Our previous findings suggest that this interacting partner is unlikely to be tau and may be a different protein (perhaps a different MAP) that remains unidentified. Instead, it appears that tau more likely modulates PP1γ and PP1α *in situ.*

The RVxF motif is one of the most common binding sequences for PP1-interacting partners. Tau contains three RVxF-like PP1-binding motifs, of which two are within the MTBR (aa 343–346 and 375–378), and one is within the extreme N-terminus (aa 5–8). However, there are several other docking sites on PP1 that could be involved in modulating its interaction and activation by tau. To address this question, we characterized the association of WT tau protein with PP1α and PP1γ by measuring phosphatase interactions with different domains within tau. The MTBRs of tau showed the strongest protein–protein interaction with PP1, while the termini (N- or C-) did not significantly alter the interaction with WT tau. These data are consistent with our recent findings showing that a mutation within the MTBR (i.e. P301L) strongly enhances PP1 binding and activity, while an N-terminal PAD mutation (i.e. R5L) increases activity but not binding [9]. Previous studies suggested that tau helped localize PP1 to microtubules which seems somewhat incompatible with PP1 also binding to tau's MTBR domain. However, whether the entire MTBR and flanking regions are completely inaccessible when tau is bound to microtubules is not entirely clear. Data suggest that the MTBR flanking regions are critical to targeting the MTBRs to interact with microtubules, allowing some domains within the MTBR to remain highly flexible and interact dynamically, while others become rigid and stably interact [52–54]. Perhaps subregions within the MTBR/flanking residues are capable of binding both PP1 and microtubules simultaneously. Another possibility is that PP1 binding partners often bind to PP1 at multiple sites utilizing a variety of different interacting domains. Indeed, so-called intrinsically disordered proteins (like tau) are highly represented in the group of PP1-interacting proteins [19], which is likely due to their heightened flexibility and ability to dynamically interact with binding partners (discussed further below). Perhaps when tau is microtubule-bound it interacts through a different motif than when it is unbound from microtubules. Recent
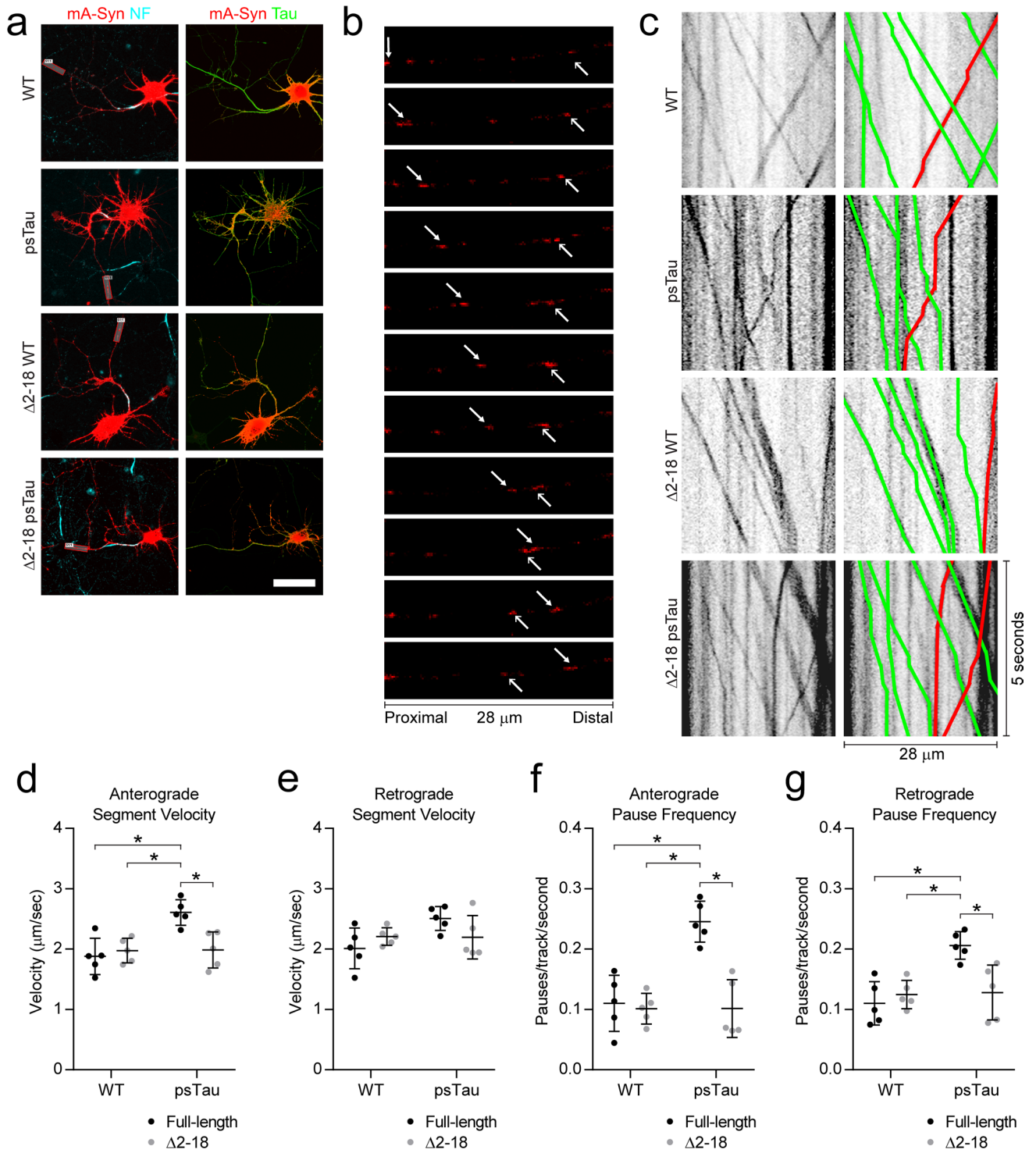
data also suggest the tau-microtubule interaction is highly dynamic with dwell times of ~ 40 ms [55], which could help facilitate such complex dynamic tau-PP1 interaction on and off microtubules. Finally, there could be an additional, yet unidentified, interacting partner that is important for tau-mediated tethering of the tau-PP1 complex to microtubules. Importantly, our prior studies in squid axoplasm assays clearly demonstrate microtubule binding is not a requirement for pathological forms of tau to trigger axonal transport impairment via the PP1 mechanism [24, 41, 45].

The lack of stable higher order structures or prevalence of low complexity domains in many PP1 regulatory proteins, like tau, may have important mechanistic implications and allow interaction between multiple sites and motifs [56,

◂**Fig. 5** psTau alters normal axonal transport in primary rat neurons dependent on PAD. **a** Primary rat hippocampal neurons were co-transfected with fluorescent-tagged synaptophysin (mA-syn, red) and a tau construct (WT tau, psTau, Δ2–18 tau, or Δ2–18 psTau). Axons were labeled in live cells (left panels) using an antibody that recognizes an external domain of neurofascin (cyan) in the axon initial segment. The boxes represent the stimulation areas that were bleached and imaged to create the live movies of transport in the axon. Co-expression of tau (green) and mA-syn (red) was confirmed with post-fixation immunostaining (right panels). Scale bar represents 50 μm. **b** Confocal microscopy was used to generate live cell movies of mA-syn transport at ~28 frames/second. Each panel image is one second after the previous panel. Transport of mA-syn was observed in the anterograde (solid arrowhead) and retrograde (barbed arrowhead) directions. **c** Kymographs were generated and analyzed using the KymoAnalyzer ImageJ macro. Anterograde transport is shown in green and retrograde transport is shown in red. **d** psTau increased anterograde segment velocity compared to all other tau constructs. **e** No significant differences in retrograde segment velocity were detected among the tau constructs. **f** Expression of psTau resulted in a significant increase in pause frequency of mA-Syn traveling in the anterograde direction compared to all other conditions. **g** psTau also increased retrograde pause frequency compared to expression of the other tau constructs. These experiments were repeated 5 independent times and data represent the mean ± SD. *$p \leq 0.05$ in a two-way ANOVA with Tukey's post hoc test with psTau modification and Δ2-18 deletion as the two factors

57]. Interacting partners bind to PP1 along surface grooves that recognize motifs like RVxF but binding alone does not always affect the catalytic site or change PP1 activity as the two sites are separated by ~20 Å [19]. Tau also could play a role in modulating substrate specificity by blocking or promoting substrate binding and/or access to the active site in PP1, but further work is required to test these hypotheses. Despite the disordered nature of many PP1-interacting proteins, pre-formed secondary structures, particularly α-helices, are important for binding to PP1 [57]. The TNT1 antibody detects a conformation-specific epitope in PAD which may indicate that the predicted α-helix in that region is important for functional interactions with PP1 [25, 58].

The salience of the PAD within the extreme amino terminus of tau was demonstrated, by our group, in multiple ways using the squid axoplasm model system. Without PAD present, tau aggregates, N-terminal tau fragments, psTau monomers and FTDP-17 mutant tau monomers do not significantly impair axonal transport, while a synthetic PAD peptide was sufficient to significantly impair axonal transport [9, 24, 41, 45]. Together, these studies highlighted the necessity and sufficiency of the N-terminal PAD for tau-mediated transport impairment. Subsequently, we tested whether deleting PAD would directly impact the interaction and activation of PP1 by WT and psTau. Deletion of PAD from psTau reduced the interaction with and activation of PP1γ but did not significantly impact interaction or activation with WT tau. In addition, PAD deletion eliminates tau-induced increases in active PP1 and rescues the increase in pause frequency induced by psTau expression (discussed

further below) in primary mammalian neurons. These data support prior findings demonstrating the importance of PAD in tau-induced transport impairment.

The landscape of protein phosphatase-mediated tau dephosphorylation is complex as tau may serve as substrate for and regulator of phosphatases. Indeed, there may be a role for PP1, PP2A, PP2B and PP5 in the modulation of tau phosphorylation in normal physiology and pathology, and different phosphatases appear to show distinct site preferences [59–62]. Specifically, the sites under investigation here with psTau (S199/S202/T205), are not effectively dephosphorylated by PP1 in AD-derived insoluble phospho-tau samples [59, 60]. However, in recombinant protein studies *in vitro*, PP1 can dephosphorylate T205 well and is less effective at S199 and S202. Generally, the data support that other phosphatases, including PP2A, PP2B and PP5 are more effective at dephosphorylating tau at these sites [59, 60]. The psTau modifications enhanced tau interaction with PP1γ in our assays. Given the weak dephosphorylation of two of these sites by PP1, the increased protein–protein interaction that may occur when tau is phosphorylated at this sight is likely driven more by changes to tau conformation rather than PP1-mediated dephosphorylation. Dephosphorylation of tau also may affect tau's normal function, including its affinity for microtubule binding. The downstream effects this might exert on transport along the axon is not known but supraphysiological saturation of microtubules with WT tau did not alter axonal transport in squid axoplasm [63].

Implications of the Tau-PP1 Interaction in Tauopathies

Prior studies using a squid axoplasm model show that abnormal tau species, associated with AD and other tauopathies, cause transport defects that are mediated by PAD-induced abnormal activation of a regulatory signaling pathway involving PP1-induced activation of GSK3β and subsequent phosphorylation of kinesin light chain [24, 41, 45, 47, 63, 64]. These abnormal forms of tau include those displaying increased phosphorylation and conformational changes (e.g. PAD exposure and oligomerization), that are associated with synapse [65, 66] and axon degeneration [67, 68], and correlate with cognitive decline during disease progression [27, 69–71]. Toxic activation of this signaling pathway is consistent with other studies indicating amyloid β-induced axonal transport defects depended on tau and GSK3β activity in a cultured neuron model [72]. GSK3β activity is increased in AD but relatively little is known about changes to PP1 isoform activity [73, 74]. Total PP1 activity is somewhat decreased in some studies but to a lesser extent than other well-known tau phosphatases like PP2A [75–77].

Several studies have highlighted the prominent role of PP2A as a main tau phosphatase, as well as the connections

between tau phosphorylation, PP2A levels/activity, and AD pathology (reviewed in [62, 78, 79]). Data presented here on PP1 and prior work with PP2A show that both phosphatases bind tau in the region of the MTBRs [80]. The apparent overlap in binding regions may suggest some competition between these two phosphatases, which could be reminiscent of the competition between Fyn and PP2A for binding to tau or MAP2 and tau for binding to PP2A [81]. Interestingly, PP2A activity, mRNA and protein levels are decreased in human AD brains, which could facilitate tau-PP1 interactions [77]. Published data also suggests PP2A provides ~71% of tau phosphatase activity in the brain, while PP1 provides only ~11% [59]. Perhaps this differential reflects tau as an effective substrate for PP2A but also as a regulator of PP1 localization and activity. This hypothesis would also support the strong inverse correlation between PP2A deficits and accumulation of phospho-tau in human disease, with only mild changes in PP1 activity [75–77]. Interestingly, FTDP-17 mutant tau, including P301L, shows reduced PP2A binding [82], but our recent work finds the opposite for this mutant tau binding to PP1 [9].

The data presented here, and prior findings suggest that phosphorylation of tau at the AT8 sites is one that alters tau conformation, exposes PAD and disrupts axonal function. One of the earliest signs of abnormal tau deposition in human brains is called pretangle pathology, which is diffuse granular cytoplasmic deposits that extend into connected processes and precedes the formation of more compact inclusions that ultimately coalesce into mature tangles (all of which remain AT8 + through all disease stages) [25, 33, 83, 84]. The AT8 antibody is widely used for Braak staging AD neuropathology (due to its ability to detect the range of inclusion stages and sensitivity) and AT8 + tau is a prominent pretangle modification in AD [24, 27, 30–34], implying it may start acting at the early stages of tau-mediated pathogenesis. More recently, we found that AT8 phosphorylation and PAD exposure occur initially in axons of the mossy fiber and Schaffer collateral pathways prior to the appearance of cell body inclusions in cognitively intact and mild cognitive impairment patients [85]. Early work described the AT8 epitope as phosphorylation at S199 and S202 [28], but a subsequent paper showed that T205 was also part of the AT8 phosphoepitope [86]. More recent evidence suggests AT8 recognizes phosphorylation at a combination of sites that can include S198, S199, S202, T205, S208, and/or S210 [29]. Despite a lack of strict specificity of the AT8 antibody epitope, structural FRET studies clearly showed that simultaneous pseudophosphorylation specifically at S199, S202 and T205 (glutamic acid mutations were used, same as psTau used here) alters soluble tau structure leading to exposure of the N-terminus [23]. psTau modifications also reduce microtubule binding affinity [87] and impair

axonal transport through a PP1-mediated mechanism in squid axoplasm [24]. Thus, our focus on this triple modification here was due specifically to these known structural changes (not an antibody epitope per se) and we confirmed this by showing that psTau aberrantly exposes PAD in non-denaturing dot blots of recombinant psTau monomers. Recent data suggests specific single or other combinations of phosphomimetic modifications in this region of tau may alter its effects on axonal transport in the squid axoplasm [35]. Future studies are required to translate these effects to mammalian neurons. However, the status of PAD exposure in the individual or alternative combinations of modifications in this region of tau are not yet defined.

Based on the known effect of phosphomimics at S199, S202 and T205 on the N-terminus of tau, we explored its effect on the functional interactions with PP1 and its impact on axonal transport in mammalian neurons. The psTau modification significantly enhanced the interaction with PP1γ, compared to WT tau, and its expression increased levels of active PP1γ in cells. Perfusion of psTau monomers significantly impaired axonal transport in the squid axoplasm [24], but whether this effect translated into mammalian neurons remained unexplored. Using rat primary hippocampal neurons, we found that expression of wild-type tau does not significantly alter axonal transport velocity or pause frequencies, which is consistent with prior work showing wild-type tau does not impair transport in squid axoplasm (up to 20 times physiological levels) [63], primary rat hippocampal neurons [9], or tau-overexpressing transgenic mice [88]. In contrast to WT tau, psTau robustly increased pause frequencies (anterograde and retrograde) in a PAD-dependent fashion (deletion rescued transport disruption), and removal of PAD from psTau significantly reduced PP1γ binding and activation of PP1γ. We also found that psTau increased anterograde transport velocity of synaptophysin-labeled vesicles, which was not observed previously in the squid axoplasm assay [24]. These differences in the findings are likely due to the methods for imaging and measuring transport in each assay. In the squid, transport rate measurements are a function of both transport rate and frequency of cargoes entering and exiting the focal plane (detailed in [9, 89]). As a result, mechanisms slowing the average rate of cargo transport (e.g. affecting motor ATPase activity) or reducing the frequency of organelles entering or exiting the focal plane (e.g. cargo dissociation) produce a similar readout of slower transport rate in the squid axoplasm assay [9, 89]. In contrast, the fluorescence labeling of cargo-associated proteins (such as synaptophysin used here) and live-cell confocal microscopy allows for direct measurement of transport velocity and cargo pausing separately. In addition, anterograde cargo pause frequency increased 123% in psTau expressing primary neurons versus WT tau expressing neurons, while anterograde velocity increased only ~38% in

psTau neurons over WT tau neurons. Perhaps the combination of different imaging modalities and the more robust effect on cargo pausing overshadowed a mild increase in anterograde transport rate in our prior squid axoplasm studies. Together, the data suggest that phosphorylation in the S199-T205 region, a post-translational modification of tau closely tied to early pathology in AD and other tauopathies, may drive axonal transport dysfunction as a monomeric protein through a PP1-dependent mechanism and that PAD is an important component of this effect [24].

Conclusions

Collectively, published work and the current results suggest that the phosphorylation at residues associated with the AT8 sites occurs first in axons during early disease, may lead to aberrant PAD exposure, and abnormal interaction and activation of PP1γ, resulting in axonal transport impairment in a PAD-dependent fashion [24, 85]. Together, this supports the hypotheses that tau can regulate PP1 activity through a direct interaction with PP1 and disease-associated post-translational modifications of tau (such as phosphorylation within S199-T205) can modulate this function, thereby altering normal axonal transport [8, 46, 90]. The interaction with and activation of PP1 by tau occurred with both PP1α and PP1γ. Tau's MTBR appears to be the primary mediator of interaction with PP1 while the termini of tau play modulatory roles in both interaction and activation of PP1. The disease-associated psTau construct induced further increases in interaction and activity, compared to WT tau, with the PP1γ isoform only. Our recent studies with mutant tau suggest specifically that PP1γ is the key isoform for this mechanism of transport disruption [9]. Deletion of PAD reduced this interaction and its effect on active PP1γ levels. PAD deletion also rescued the psTau-induced disruption to axonal transport in primary hippocampal neurons. The evidence provided here suggests tau's functional repertoire reaches beyond modulating microtubule dynamics and includes regulating cell signaling cascades in a highly specific manner [3]. This functional effect of tau and the implications of how disease-specific modifications impact this mechanism may provide new targets for pharmacological interventions for treating tauopathies.

Declarations

References

1. Bunker JM, Wilson L, Jordan MA, Feinstein SC (2004) Modulation of microtubule dynamics by tau in living cells: implications for development and neurodegeneration. Mol Biol Cell 15(6):2720–2728. https://doi.org/10.1091/mbc.E04-01-0062

2. Qiang L, Sun X, Austin TO, Muralidharan H, Jean DC, Liu M, Yu W, Baas PW (2018) Tau Does Not Stabilize Axonal Microtubules but Rather Enables Them to Have Long Labile Domains. Curr Biol CB 28(13):2181–2189 e2184. https://doi.org/10.1016/j.cub.2018.05.045

3. Mueller RL, Combs B, Alhadidy MM, Brady ST, Morfini GA, Kanaan NM (2021) Tau: A Signaling Hub Protein. Front Mol Neurosci 14:647054. https://doi.org/10.3389/fnmol.2021.647054

4. Leugers CJ, Koh JY, Hong W, Lee G (2013) Tau in MAPK activation. Front Neurol 4:161. https://doi.org/10.3389/fneur.2013.00161

5. Leugers CJ, Lee G (2010) Tau potentiates nerve growth factor-induced mitogen-activated protein kinase signaling and neurite initiation without a requirement for microtubule binding. J Biol Chem 285(25):19125–19134. https://doi.org/10.1074/jbc.M110.105387

6. Ittner LM, Ke YD, Delerue F, Bi M, Gladbach A, van Eersel J, Wolfing H, Chieng BC et al (2010) Dendritic function of tau mediates amyloid-beta toxicity in Alzheimer's disease mouse models. Cell 142(3):387–397. https://doi.org/10.1016/j.cell.2010.06.036

7. Lee G, Newman ST, Gard DL, Band H, Panchamoorthy G (1998) Tau interacts with src-family non-receptor tyrosine kinases. J Cell Sci 111(Pt 21):3167–3177

8. Sharma VM, Litersky JM, Bhaskar K, Lee G (2007) Tau impacts on growth-factor-stimulated actin remodeling. J Cell Sci 120(Pt 5):748–757. https://doi.org/10.1242/jcs.03378

9. Combs B, Christensen KR, Richards C, Kneynsberg A, Mueller RL, Morris SL, Morfini GA, Brady ST et al (2021) Frontotemporal lobar dementia mutant tau impairs axonal transport through a protein phosphatase 1gamma-dependent mechanism. J Neurosci 41(45):9431–9451. https://doi.org/10.1523/JNEUROSCI.1914-20.2021

10. Liao H, Li Y, Brautigan DL, Gundersen GG (1998) Protein phosphatase 1 is targeted to microtubules by the microtubule-associated protein Tau. J Biol Chem 273(34):21901–21908

11. Cohen PT (2002) Protein phosphatase 1–targeted in many directions. J Cell Sci 115(Pt 2):241–256

12. Morfini GA, Burns M, Binder LI, Kanaan NM, LaPointe N, Bosco DA, Brown RH Jr, Brown H et al (2009) Axonal transport defects in neurodegenerative diseases. J Neurosci 29(41):12776–12786. https://doi.org/10.1523/JNEUROSCI.3463-09.2009

13. Ceulemans H, Bollen M (2004) Functional diversity of protein phosphatase-1, a cellular economizer and reset button. Physiol Rev 84(1):1–39. https://doi.org/10.1152/physrev.00013.2003

14. Fardilha M, Esteves SL, Korrodi-Gregorio L, da Cruz e Silva OA, da Cruz e Silva FF (2010) The physiological relevance of protein phosphatase 1 and its interacting proteins to health and disease. Curr Med Chem 17(33):3996–4017. https://doi.org/10.2174/092986710793205363

15. Ouimet CC, da Cruz e Silva EF, Greengard P (1995) The alpha and gamma 1 isoforms of protein phosphatase 1 are highly and specifically concentrated in dendritic spines. Proc Natl Acad Sci U S A 92(8):3396–3400. https://doi.org/10.1073/pnas.92.8.3396

16. Shima H, Haneji T, Hatano Y, Kasugai I, Sugimura T, Nagao M (1993) Protein phosphatase 1 gamma 2 is associated with nuclei of meiotic cells in rat testis. Biochem Biophys Res Commun 194(2):930–937. https://doi.org/10.1006/bbrc.1993.1910

17. Kitagawa Y, Sasaki K, Shima H, Shibuya M, Sugimura T, Nagao M (1990) Protein phosphatases possibly involved in rat spermatogenesis. Biochem Biophys Res Commun 171(1):230–235. https://doi.org/10.1016/0006-291x(90)91381-2

18. Korrodi-Gregorio L, Esteves SL, Fardilha M (2014) Protein phosphatase 1 catalytic isoforms: specificity toward interacting proteins. Transl Res 164(5):366–391. https://doi.org/10.1016/j.trsl.2014.07.001

19. Peti W, Nairn AC, Page R (2013) Structural basis for protein phosphatase 1 regulation and specificity. FEBS J 280(2):596–611. https://doi.org/10.1111/j.1742-4658.2012.08509.x

20. Egloff MP, Johnson DF, Moorhead G, Cohen PT, Cohen P, Barford D (1997) Structural basis for the recognition of regulatory subunits by the catalytic subunit of protein phosphatase 1. EMBO J 16(8):1876–1887. https://doi.org/10.1093/emboj/16.8.1876

21. Wakula P, Beullens M, Ceulemans H, Stalmans W, Bollen M (2003) Degeneracy and function of the ubiquitous RVXF motif that mediates binding to protein phosphatase-1. J Biol Chem 278(21):18817–18823. https://doi.org/10.1074/jbc.M300175200

22. Kneynsberg A, Combs B, Christensen K, Morfini G, Kanaan NM (2017) Axonal degeneration in tauopathies: disease relevance and underlying mechanisms. Front Neurosci 11:572. https://doi.org/10.3389/fnins.2017.00572

23. Jeganathan S, Hascher A, Chinnathambi S, Biernat J, Mandelkow EM, Mandelkow E (2008) Proline-directed pseudo-phosphorylation at AT8 and PHF1 epitopes induces a compaction of the paperclip folding of Tau and generates a pathological (MC-1) conformation. J Biol Chem 283(46):32066–32076. https://doi.org/10.1074/jbc.M805300200

24. Kanaan NM, Morfini GA, LaPointe NE, Pigino GF, Patterson KR, Song Y, Andreadis A, Fu Y et al (2011) Pathogenic forms of tau inhibit kinesin-dependent axonal transport through a mechanism involving activation of axonal phosphotransferases. J Neurosci 31(27):9858–9868. https://doi.org/10.1523/JNEUROSCI.0560-11.2011

25. Combs B, Hamel C, Kanaan NM (2016) Pathological conformations involving the amino terminus of tau occur early in Alzheimer's disease and are differentially detected by monoclonal antibodies. Neurobiol Dis 94:18–31. https://doi.org/10.1016/j.nbd.2016.05.016

26. Combs B, Kanaan NM (2017) Exposure of the amino terminus of tau is a pathological event in multiple tauopathies. Am J Pathol. https://doi.org/10.1016/j.ajpath.2017.01.019

27. Braak H, Alafuzoff I, Arzberger T, Kretzschmar H, Del Tredici K (2006) Staging of Alzheimer disease-associated neurofibrillary pathology using paraffin sections and immunocytochemistry. Acta Neuropathol 112(4):389–404. https://doi.org/10.1007/s00401-006-0127-z

28. Biernat J, Mandelkow EM, Schroter C, Lichtenberg-Kraag B, Steiner B, Berling B, Meyer H, Mercken M et al (1992) The switch of tau protein to an Alzheimer-like state includes the phosphorylation of two serine-proline motifs upstream of the microtubule binding region. Embo J 11(4):1593–1597

29. Malia TJ, Teplyakov A, Ernst R, Wu SJ, Lacy ER, Liu X, Vandermeeren M, Mercken M et al (2016) Epitope mapping and structural basis for the recognition of phosphorylated tau by the anti-tau antibody AT8. Proteins 84(4):427–434. https://doi.org/10.1002/prot.24988

30. Braak H, Braak E (1995) Staging of Alzheimer's disease-related neurofibrillary changes. Neurobiol Aging 16(3):271–278 (discussion 278-284)

31. Garcia-Sierra F, Hauw JJ, Duyckaerts C, Wischik CM, Luna-Munoz J, Mena R (2000) The extent of neurofibrillary pathology in perforant pathway neurons is the key determinant of dementia in the very old. Acta Neuropathol (Berl) 100(1):29–35

32. Luna-Munoz J, Chavez-Macias L, Garcia-Sierra F, Mena R (2007) Earliest stages of tau conformational changes are related to the appearance of a sequence of specific phospho-dependent tau epitopes in Alzheimer's disease. J Alzheimers Dis 12(4):365–375

33. Braak E, Braak H, Mandelkow EM (1994) A sequence of cytoskeleton changes related to the formation of neurofibrillary tangles and neuropil threads. Acta Neuropathol (Berl) 87(6):554–567

34. Braak H, Thal DR, Ghebremedhin E, Del Tredici K (2011) Stages of the pathologic process in Alzheimer disease: age categories from 1 to 100 years. J Neuropathol Exp Neurol 70(11):960–969. https://doi.org/10.1097/NEN.0b013e318232a379

35. Morris SL, Tsai MY, Aloe S, Bechberger K, Konig S, Morfini G, Brady ST (2020) Defined tau phosphospecies differentially inhibit fast axonal transport through activation of two independent signaling pathways. Front Mol Neurosci 13:610037. https://doi.org/10.3389/fnmol.2020.610037

36. Morris SL, Brady ST (2022) Tau phosphorylation and PAD exposure in regulation of axonal growth. Front Cell Dev Biol 10:1023418. https://doi.org/10.3389/fcell.2022.1023418

37. Machleidt T, Woodroofe CC, Schwinn MK, Mendez J, Robers MB, Zimmerman K, Otto P, Daniels DL et al (2015) NanoBRET–A novel BRET platform for the analysis of protein-protein interactions. ACS Chem Biol 10(8):1797–1804. https://doi.org/10.1021/acschembio.5b00143

38. Combs B, Tiernan CT, Hamel C, Kanaan NM (2017) Production of recombinant tau oligomers in vitro. Methods Cell Biol 141:45–64. https://doi.org/10.1016/bs.mcb.2017.06.005

39. Cox K, Combs B, Abdelmesih B, Morfini G, Brady ST, Kanaan NM (2016) Analysis of isoform-specific tau aggregates suggests a common toxic mechanism involving similar pathological conformations and axonal transport inhibition. Neurobiol Aging 47:113–126. https://doi.org/10.1016/j.neurobiolaging.2016.07.015

40. Berry RW, Sweet AP, Clark FA, Lagalwar S, Lapin BR, Wang T, Topgi S, Guillozet-Bongaarts AL, Cochran EJ, Bigio EH, Binder LI (2004) Tau epitope display in progressive supranuclear palsy and corticobasal degeneration. J Neurocytol 33(3):287–295. https://doi.org/10.1023/B:NEUR.0000044190.96426.b9

41. Kanaan NM, Morfini G, Pigino G, LaPointe NE, Andreadis A, Song Y, Leitman E, Binder LI et al (2012) Phosphorylation in the amino terminus of tau prevents inhibition of anterograde axonal transport. Neurobiol Aging 33 (4):826 e815–830. https://doi.org/10.1016/j.neurobiolaging.2011.06.006

42. Grabinski TM, Kneynsberg A, Manfredsson FP, Kanaan NM (2015) A method for combining RNAscope in situ hybridization

with immunohistochemistry in thick free-floating brain sections and primary neuronal cultures. PLoS One 10(3):e0120120. https://doi.org/10.1371/journal.pone.0120120

43. Hedstrom KL, Ogawa Y, Rasband MN (2008) AnkyrinG is required for maintenance of the axon initial segment and neuronal polarity. J Cell Biol 183(4):635–640. https://doi.org/10.1083/jcb.200806112

44. Neumann S, Chassefeyre R, Campbell GE, Encalada SE (2017) KymoAnalyzer: a software tool for the quantitative analysis of intracellular transport in neurons. Traffic 18(1):71–88. https://doi.org/10.1111/tra.12456

45. LaPointe NE, Morfini G, Pigino G, Gaisina IN, Kozikowski AP, Binder LI, Brady ST (2009) The amino terminus of tau inhibits kinesin-dependent axonal transport: implications for filament toxicity. J Neurosci Res 87(2):440–451. https://doi.org/10.1002/jnr.21850

46. Kanaan NM, Pigino GF, Brady ST, Lazarov O, Binder LI, Morfini GA (2013) Axonal degeneration in Alzheimer's disease: when signaling abnormalities meet the axonal transport system. Exp Neurol 246:44–53. https://doi.org/10.1016/j.expneurol.2012.06.003

47. Morfini G, Szebenyi G, Brown H, Pant HC, Pigino G, DeBoer S, Beffert U, Brady ST (2004) A novel CDK5-dependent pathway for regulating GSK3 activity and kinesin-driven motility in neurons. EMBO J 23(11):2235–2245. https://doi.org/10.1038/sj.emboj.7600237

48. Dohadwala M, da Cruz e Silva EF, Hall FL, Williams RT, Carbonaro-Hall DA, Nairn AC, Greengard P, Berndt N (1994) Phosphorylation and inactivation of protein phosphatase 1 by cyclin-dependent kinases. Proc Natl Acad Sci U S A 91(14):6408–6412. https://doi.org/10.1073/pnas.91.14.6408

49. Hou H, Sun L, Siddoway BA, Petralia RS, Yang H, Gu H, Nairn AC, Xia H (2013) Synaptic NMDA receptor stimulation activates PP1 by inhibiting its phosphorylation by Cdk5. J Cell Biol 203(3):521–535. https://doi.org/10.1083/jcb.201303035

50. Strack S, Kini S, Ebner FF, Wadzinski BE, Colbran RJ (1999) Differential cellular and subcellular localization of protein phosphatase 1 isoforms in brain. J Comp Neurol 413(3):373–384

51. Bordelon JR, Smith Y, Nairn AC, Colbran RJ, Greengard P, Muly EC (2005) Differential localization of protein phosphatase-1alpha, beta and gamma1 isoforms in primate prefrontal cortex. Cereb Cortex 15(12):1928–1937. https://doi.org/10.1093/cercor/bhi070

52. Mukrasch MD, von Bergen M, Biernat J, Fischer D, Griesinger C, Mandelkow E, Zweckstetter M (2007) The "jaws" of the tau-microtubule interaction. J Biol Chem 282(16):12230–12239. https://doi.org/10.1074/jbc.M607159200

53. El Mammeri N, Dregni AJ, Duan P, Wang HK, Hong M (2022) Microtubule-binding core of the tau protein. Sci Adv 8(29):eabo4459. https://doi.org/10.1126/sciadv.abo4459

54. Kellogg EH, Hejab NMA, Poepsel S, Downing KH, DiMaio F, Nogales E (2018) Near-atomic model of microtubule-tau interactions. Science 360(6394):1242–1246. https://doi.org/10.1126/science.aat1780

55. Janning D, Igaev M, Sundermann F, Bruhmann J, Beutel O, Heinisch JJ, Bakota L, Piehler J et al (2014) Single-molecule tracking of tau reveals fast kiss-and-hop interaction with microtubules in living neurons. Mol Biol Cell 25(22):3541–3551. https://doi.org/10.1091/mbc.E14-06-1099

56. Bollen M, Peti W, Ragusa MJ, Beullens M (2010) The extended PP1 toolkit: designed to create specificity. Trends Biochem Sci 35(8):450–458. https://doi.org/10.1016/j.tibs.2010.03.002

57. Choy MS, Page R, Peti W (2012) Regulation of protein phosphatase 1 by intrinsically disordered proteins. Biochem Soc Trans 40(5):969–974. https://doi.org/10.1042/BST20120094

58. Gamblin TC (2005) Potential structure/function relationships of predicted secondary structural elements of tau. Biochim Biophys Acta 1739(2–3):140–149

59. Liu F, Grundke-Iqbal I, Iqbal K, Gong CX (2005) Contributions of protein phosphatases PP1, PP2A, PP2B and PP5 to the regulation of tau phosphorylation. Eur J Neurosci 22(8):1942–1950. https://doi.org/10.1111/j.1460-9568.2005.04391.x

60. Rahman A, Grundke-Iqbal I, Iqbal K (2005) Phosphothreonine-212 of Alzheimer abnormally hyperphosphorylated tau is a preferred substrate of protein phosphatase-1. Neurochem Res 30(2):277–287

61. Liu F, Iqbal K, Grundke-Iqbal I, Rossie S, Gong CX (2005) Dephosphorylation of tau by protein phosphatase 5: impairment in Alzheimer's disease. J Biol Chem 280(3):1790–1796. https://doi.org/10.1074/jbc.M410775200

62. Martin L, Latypova X, Wilson CM, Magnaudeix A, Perrin ML, Terro F (2013) Tau protein phosphatases in Alzheimer's disease: the leading role of PP2A. Ageing Res Rev 12(1):39–49. https://doi.org/10.1016/j.arr.2012.06.008

63. Morfini G, Pigino G, Mizuno N, Kikkawa M, Brady ST (2007) Tau binding to microtubules does not directly affect microtubule-based vesicle motility. J Neurosci Res 85(12):2620–2630. https://doi.org/10.1002/jnr.21154

64. Morfini G, Szebenyi G, Elluru R, Ratner N, Brady ST (2002) Glycogen synthase kinase 3 phosphorylates kinesin light chains and negatively regulates kinesin-based motility. EMBO J 21(3):281–293. https://doi.org/10.1093/emboj/21.3.281

65. DeKosky ST, Scheff SW (1990) Synapse loss in frontal cortex biopsies in Alzheimer's disease: correlation with cognitive severity. Ann Neurol 27(5):457–464. https://doi.org/10.1002/ana.410270502

66. Masliah E, Hansen L, Albright T, Mallory M, Terry RD (1991) Immunoelectron microscopic study of synaptic pathology in Alzheimer's disease. Acta Neuropathol 81(4):428–433

67. Bell KF, Claudio Cuello A (2006) Altered synaptic function in Alzheimer's disease. Eur J Pharmacol 545(1):11–21. https://doi.org/10.1016/j.ejphar.2006.06.045

68. Vana L, Kanaan NM, Ugwu IC, Wuu J, Mufson EJ, Binder LI (2011) Progression of tau pathology in cholinergic Basal forebrain neurons in mild cognitive impairment and Alzheimer's disease. Am J Pathol 179(5):2533–2550. https://doi.org/10.1016/j.ajpath.2011.07.044

69. Braak H, Braak E (1991) Neuropathological stageing of Alzheimer-related changes. Acta Neuropathol 82(4):239–259

70. Giannakopoulos P, Herrmann FR, Bussiere T, Bouras C, Kovari E, Perl DP, Morrison JH, Gold G et al (2003) Tangle and neuron numbers, but not amyloid load, predict cognitive status in Alzheimer's disease. Neurology 60(9):1495–1500

71. Arriagada PV, Growdon JH, Hedley-Whyte ET, Hyman BT (1992) Neurofibrillary tangles but not senile plaques parallel duration and severity of Alzheimer's disease. Neurology 42(3 Pt 1):631–639

72. Vossel KA, Xu JC, Fomenko V, Miyamoto T, Suberbielle E, Knox JA, Ho K, Kim DH et al (2015) Tau reduction prevents Abeta-induced axonal transport deficits by blocking activation of GSK-3beta. J Cell Biol 209(3):419–433. https://doi.org/10.1083/jcb.201407065

73. Pei JJ, Braak E, Braak H, Grundke-Iqbal I, Iqbal K, Winblad B, Cowburn RF (1999) Distribution of active glycogen synthase kinase 3beta (GSK-3beta) in brains staged for Alzheimer disease neurofibrillary changes. J Neuropathol Exp Neurol 58(9):1010–1019

74. Leroy K, Yilmaz Z, Brion JP (2007) Increased level of active GSK-3beta in Alzheimer's disease and accumulation in argyrophilic grains and in neurones at different stages of neurofibrillary degeneration. Neuropathol Appl Neurobiol 33(1):43–55

75. Gong CX, Shaikh S, Wang JZ, Zaidi T, Grundke-Iqbal I, Iqbal K (1995) Phosphatase activity toward abnormally phosphorylated tau: decrease in Alzheimer disease brain. J Neurochem 65(2):732–738

76. Gong CX, Singh TJ, Grundke-Iqbal I, Iqbal K (1993) Phosphoprotein phosphatase activities in Alzheimer disease brain. J Neurochem 61(3):921–927

77. Sontag E, Luangpirom A, Hladik C, Mudrak I, Ogris E, Speciale S, White CL 3rd (2004) Altered expression levels of the protein phosphatase 2A ABalphaC enzyme are associated with Alzheimer

disease pathology. J Neuropathol Exp Neurol 63(4):287–301. https://doi.org/10.1093/jnen/63.4.287

78. Sontag JM, Sontag E (2014) Protein phosphatase 2A dysfunction in Alzheimer's disease. Front Mol Neurosci 7:16. https://doi.org/10.3389/fnmol.2014.00016

79. Taleski G, Sontag E (2018) Protein phosphatase 2A and tau: an orchestrated "Pas de Deux." FEBS Lett 592(7):1079–1095. https://doi.org/10.1002/1873-3468.12907

80. Sontag E, Nunbhakdi-Craig V, Lee G, Brandt R, Kamibayashi C, Kuret J, White CL 3rd, Mumby MC et al (1999) Molecular interactions among protein phosphatase 2A, tau, and microtubules. Implications for the regulation of tau phosphorylation and the development of tauopathies. J Biol Chem 274(36):25490–25498

81. Sontag JM, Nunbhakdi-Craig V, White CL 3rd, Halpain S, Sontag E (2012) The protein phosphatase PP2A/Balpha binds to the microtubule-associated proteins Tau and MAP2 at a motif also recognized by the kinase Fyn: implications for tauopathies. J Biol Chem 287(18):14984–14993. https://doi.org/10.1074/jbc.M111.338681

82. Goedert M, Satumtira S, Jakes R, Smith MJ, Kamibayashi C, White CL 3rd, Sontag E (2000) Reduced binding of protein phosphatase 2A to tau protein with frontotemporal dementia and parkinsonism linked to chromosome 17 mutations. J Neurochem 75(5):2155–2162. https://doi.org/10.1046/j.1471-4159.2000.0752155.x

83. Bancher C, Brunner C, Lassmann H, Budka H, Jellinger K, Wiche G, Seitelberger F, Grundke-Iqbal I, Iqbal K et al (1989) Accumulation of abnormally phosphorylated tau precedes the formation of neurofibrillary tangles in Alzheimer's disease. Brain Res 477(1–2):90–99

84. Bancher C, Grundke-Iqbal I, Iqbal K, Fried VA, Smith HT, Wisniewski HM (1991) Abnormal phosphorylation of tau precedes ubiquitination in neurofibrillary pathology of Alzheimer disease. Brain Res 539(1):11–18

85. Christensen KR, Beach TG, Serrano GE, Kanaan NM (2019) Pathogenic tau modifications occur in axons before the somatodendritic compartment in mossy fiber and Schaffer collateral pathways. Acta Neuropathol Commun 7(1):29. https://doi.org/10.1186/s40478-019-0675-9

86. Goedert M, Jakes R, Vanmechelen E (1995) Monoclonal antibody AT8 recognises tau protein phosphorylated at both serine 202 and threonine 205. Neurosci Lett 189(3):167–169

87. Sun Q, Gamblin TC (2009) Pseudohyperphosphorylation causing AD-like changes in tau has significant effects on its polymerization. Biochemistry 48:6002–6011

88. Yuan A, Kumar A, Peterhoff C, Duff K, Nixon RA (2008) Axonal transport rates in vivo are unaffected by tau deletion or overexpression in mice. J Neurosci 28(7):1682–1687

89. Song Y, Kang M, Morfini G, Brady ST (2016) Fast axonal transport in isolated axoplasm from the squid giant axon. Methods Cell Biol 131:331–348. https://doi.org/10.1016/bs.mcb.2015.07.004

90. Souter S, Lee G (2010) Tubulin-independent tau in Alzheimer's disease and cancer: implications for disease pathogenesis and treatment. Curr Alzheimer Res 7(8):697–707. https://doi.org/10.2174/156720510793611637